

Log-Aesthetic Space Curve Segments

Norimasa Yoshida^{*}
Nihon University

Ryo Fukuda
Nihon University

Takafumi Saito[†]
Tokyo University of
Agriculture and Technology

ABSTRACT

For designing aesthetic surfaces, such as the car bodies, it is very important to use aesthetic curves as characteristic lines. In such curves, the curvature should be monotonically varying, since it dominates the distortion of reflected images on curved surfaces. In this paper, we present an interactive control method of log-aesthetic space curves. We define log-aesthetic space curves to be curves whose logarithmic curvature and torsion graphs are both linear. The linearity of these graphs constrains that the curvature and torsion are monotonically varying. We clarify the characteristics of log-aesthetic space curves and identify their family. Moreover, we present a novel method for drawing a log-aesthetic space curve segment by specifying two endpoints, their tangents, the slopes, α and β , of straight lines of the logarithmic curvature and torsion graphs, and the torsion parameter Ω . Our implementation shows that log-aesthetic curve segments can be controlled fully interactively.

Categories and Subject Descriptors

I.3.5 [Computational Geometry and Object Modeling]: Curve, surface, solid, and object representations; J.6 [COMPUTER-AIDED ENGINEERING]: Computer-aided design (CAD)

General Terms

Algorithms

Keywords

logarithmic curvature graph, logarithmic torsion graph, log-aesthetic space curves

1. INTRODUCTION

For designing aesthetic surfaces, such as the car bodies, it is very important to use aesthetic curves as characteristic

lines. In such aesthetic curves, designers usually use curvature plots to see the shape of the curve. In conventional free-form curves, such as NURBS or Bézier curves, it is difficult to control the variation of curvature by moving their control points. For planar curves, we have proposed log-aesthetic curves (formerly called aesthetic curves) [18] and its approximation by rational cubic Bézier curves [19]. Log-aesthetic curves are curves whose logarithmic curvature graphs are linear. Logarithmic curvature graphs were originally proposed by Harada [8, 9]. Harada has analyzed curvature variation properties of curves in existing aesthetic objects and discovered that their logarithmic curvature graphs are linear. The general formula of log-aesthetic space curves has been derived by Miura [13]. Note that the term "logarithmic curvature" has been used by Farouki et al in [5]. We use the term in an entirely different context. Comparing other work for generating curves with monotonically varying curvature, such as [10][6][16][17], the variation of curvature can be controlled by one parameter α in log-aesthetic curves.

For space curves with monotonically varying curvature, very little work seem to exist for directly generating them. Adams proposed a method for drawing a space curve with linearly increasing and then linearly decreasing curvature and torsion by specifying endpoint conditions [1]. In the automobile industry, space curves are usually generated as the intersection of two surfaces that are swept by two planar curves. There is no guarantee, however, that the curvature of the generated space curve is monotonically varying even if the curvature of the planar curves are monotonically varying. Farin recently proposed class A Bézier curves with monotonically varying curvature and torsion [4]. Fukuda et.al have proposed a method for drawing 3D class A Bézier curves by specifying two endpoints and their tangents [7]. As long as we know, no method exists for directly generating space curves with monotonically varying curvature and torsion, where the variations of curvature and torsion can be simply modified.

Minimum energy curves (MECs) or minimum variation curves (MVCs) [14] are widely used for designing fair curves. MECs minimize total curvature and tend to yield a large range of curvatures. MVCs minimize inline curvature changes and tend to yield a narrow range of curvatures [11]. In both of them, the user cannot directly control the variation of curvature.

In this paper, we extend the work of log-aesthetic planar

^{*}norimasa@acm.org

[†]txsaito@cc.tuat.ac.jp

curves[18] to log-aesthetic space curves. We clarify the characteristics of log-aesthetic space curves and identify their family by classifying the overall shapes of log-aesthetic space curves depending on the arc length toward the point at 0 or infinite curvature or torsion, and the behavior of tangent and binormal vectors toward such points. As every log-aesthetic curve is related to a circle[18], we show that every log-aesthetic space curve is related to a helix. We then present a method for controlling log-aesthetic space curve segments. Generating a space curve segment, however, is not a simple extension of the previous work[18], since we need to answer the following problems:

- (1) The tangential angle problem. In log-aesthetic planar curves, the tangential angle, which is the angle between the tangent vector and x axis, has one-to-one correspondence with the arc length. However, in 3D, we do not have such kind of relationships. Do we need to include the arc length in the optimization parameters?
- (2) The problems of an additional degree of freedom.
 - (2a) How to control a curve segment? Since space curves have torsion, we may need to specify additional parameters in addition to two endpoints and their tangents. Are they binormal vectors at two endpoints? Is it too restrictive to find a curve segment?
 - (2b) Is it possible to compute a curve segment in interactive frame rate? In log-aesthetic planar curves, we could use the bisection method to find a curve segment[18]. In 3D, however, we need three parameters (Λ , Ω , and ν) and the arc length to draw a curve. This may imply that we need an optimization of four parameters, which makes interactive control difficult.

We will answer the above problems and present a method for interactively controlling log-aesthetic curve segments. For (1), we propose a novel cone-intersection method. We need not include the arc length in the optimization parameters. For (2a), we propose to specify the torsion parameter Ω . We found that specifying binormal vectors at two endpoints is too restrictive to find a curve segment. For (2b), we show that we can find a curve segment using an optimization of two parameters. We also show that we can control curve segments fully interactively. More details will be described in Section 4.

2. LOG-AESTHETIC SPACE CURVES

In this section, we append logarithmic torsion graphs (LTGs) onto logarithmic curvature graphs (LCGs) [8, 9, 13, 18] and define log-aesthetic space curves to be curves whose LCGs and LTGs are both linear. The curvature and torsion of log-aesthetic space curves are monotonically varying due to the linearity of LCGs and LTGs. The role of torsion variations for aesthetic space curves is not clearly known. However, without giving any information about torsion variation, space curves cannot be generated. Therefore, in log-aesthetic space curves, we assume that LTGs are linear. Log-aesthetic space curves may play a role for clarifying the role of torsion variations.

We assume that both the radius of curvature ρ and the radius of torsion μ are monotonically increasing with respect

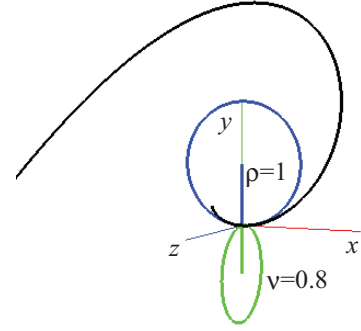


Figure 1: A log-aesthetic space curve in the standard form ($\alpha = 1$, $\beta = 1$, $\Lambda = 1$, $\Omega = 1$).

to the arc length s . This assumption will be removed later. An LCG is a graph whose horizontal and vertical axes are $\log \rho$ and $\log \rho \frac{ds}{d\rho}$, respectively. The linearity of the LCG [13, 18] is represented by

$$\log \rho \frac{ds}{d\rho} = \alpha \log \rho + c_1 \quad (1)$$

where α is the slope of the straight line and c_1 is a constant. Modifying Eq.(1) and setting $\Lambda = e^{-c_1}$, we get

$$\frac{ds}{d\rho} = \frac{\rho^{\alpha-1}}{\Lambda}. \quad (2)$$

The LTG can be obtained by replacing the radius of curvature ρ of LCGs by the radius of torsion μ . The linearity of the LTG is represented by

$$\log \mu \frac{ds}{d\mu} = \beta \log \mu + c_2 \quad (3)$$

where β is the slope of the straight line and c_2 is a constant. Modifying Eq.(3) and setting $\Omega = e^{-c_2}$, we get

$$\frac{ds}{d\mu} = \frac{\mu^{\beta-1}}{\Omega}. \quad (4)$$

To understand the overall shape of log-aesthetic space curves, we consider the standard form similarly as in log-aesthetic planar curves[18]. We first choose a reference point \mathbf{P}_r on a log-aesthetic space curve. The reference point \mathbf{P}_r can be any point of the curve except for the point at $\rho = 0$, $\rho = \infty$, $\mu = 0$ or $\mu = \infty$. We give the following constraint at the reference point.

- (1) Translation: \mathbf{P}_r is placed at the origin.
- (2) Rotation: The tangent vector at \mathbf{P}_r is parallel to $[1 \ 0 \ 0]^T$ and the main normal vector at \mathbf{P}_r is parallel to $[0 \ 1 \ 0]^T$.
- (3) Scaling: $\rho = 1$ and $\mu = \nu$ at \mathbf{P}_r .

The arc length s is set to 0 at \mathbf{P}_r . For any log-aesthetic space curve, its standard form can be obtained by an appropriate transformation, which is a composition of a translation, a rotation and a scaling. We use the standard form to identify the overall shapes of log-aesthetic space curves. See Fig.1.

Integrating Eq.(2) with respect to ρ by setting $\rho = 1$ at $s = 0$ and solving the equation for ρ , we get

$$\rho = \begin{cases} e^{\Lambda s} & \text{if } \alpha = 0 \\ (\Lambda\alpha s + 1)^{\frac{1}{\alpha}} & \text{otherwise} \end{cases} \quad (5)$$

Eq.(5) is the intrinsic equation of log-aesthetic planar curves. Similarly, integrating Eq.(4) with respect to μ by setting $\mu = \nu$ at $s = 0$ and solving the equation for μ , we get

$$\mu = \begin{cases} e^{(\Omega s + \log \nu)} & \text{if } \beta = 0 \\ (\Omega\beta s + \nu^\beta)^{\frac{1}{\beta}} & \text{otherwise} \end{cases} \quad (6)$$

Eq.(6) is monotonically increasing radius of torsion with respect to s . The equation of monotonically decreasing radius of torsion is

$$\mu = \begin{cases} e^{(-\Omega s + \log \nu)} & \text{if } \beta = 0 \\ (-\Omega\beta s + \nu^\beta)^{\frac{1}{\beta}} & \text{otherwise} \end{cases} \quad (7)$$

We define log-aesthetic space curves to be curves whose functions of the radius of curvature and the radius of torsion are Eq.(5) and Eq.(6) (or Eq.(7)), respectively. From the fundamental theorem of the local theory of curves in differential geometry[2], a curve is uniquely defined under a rigid motion if its curvature and torsion functions are specified. Thus Eq.(5) and Eq.(6) (or Eq.(7)) uniquely define space curves. In log-aesthetic space curves, the function of the radius of curvature is always Eq.(5). The function of the radius of torsion is either Eq.(6) or Eq.(7). We call the curves whose function of the radius of torsion is Eq.(6) ‘type 1’ curves. The curves whose function of the radius of torsion is Eq.(7) is called ‘type 2’ curves. In ‘type 1’ log-aesthetic space curves, both the radius of curvature and the radius of torsion are monotonically increasing with respect to the arc length. In ‘type 2’ log-aesthetic space curves, the radius of curvature is monotonically increasing whereas the radius of torsion is monotonically decreasing. Curves with monotonically decreasing radius of curvature and radius of torsion are the reparameterization of ‘type 1’ curves. Similarly, curves with monotonically decreasing radius of curvature but monotonically increasing radius of torsion is the reparameterization of ‘type 2’ curves.

In log-aesthetic planar curves, the range of arc length s is constrained only by the radius of curvature. In log-aesthetic space curves, the range of s is constrained by both the radius of curvature ρ and the radius of torsion μ . Since both ρ and μ take values between 0 to ∞ , s may have bounds depending on α and β . The value of the bound depends on α , Λ , β , Ω and ν . Fig.2 shows the bounds of s . For example, Fig.2(a) shows that ρ becomes ∞ at $s = -\frac{1}{\Lambda\alpha}$ if $\alpha < 0$. In both ‘type 1’ and ‘type 2’ curves, ρ can be 0 at the lower bound of s and ρ can be ∞ at the upper bound. In ‘type 1’ curves, μ can be 0 at the lower bound and μ can be ∞ at the upper bound. In ‘type 2’ curves, μ can be ∞ at the lower bound and μ can be 0 at the upper bound. In ‘type 1’ curves, the range of s is constrained by Fig.2(a) and (b). In ‘type 2’ curves, the range of s is constrained by Fig.2(a) and (c). In ‘type 1’ curves of $\alpha > 0$ and $\beta < 0$, the valid range of s is $-\frac{1}{\Lambda\alpha} < s < -\frac{\nu^\beta}{\Omega\beta}$. Thus the arc length of the curve is finite if both Λ and Ω are greater than 0, though the arc length can be arbitrarily large depending on Λ and Ω .

	LB	UB
$\alpha < 0$	$-\infty$	$-1/(\Lambda\alpha)$
$\alpha = 0$	$-\infty$	∞
$\alpha > 0$	$-1/(\Lambda\alpha)$	∞

(a) The Lower Bound(LB) and Upper bound(UB) of s in Eq.(5)

	LB	UB		LB	UB
$\beta < 0$	$-\infty$	$-\nu^\beta / (\Omega\beta)$	$\beta < 0$	$\nu^\beta / (\Omega\beta)$	∞
$\beta = 0$	$-\infty$	∞	$\beta = 0$	$-\infty$	∞
$\beta > 0$	$-\nu^\beta / (\Omega\beta)$	∞	$\beta > 0$	$-\infty$	$\nu^\beta / (\Omega\beta)$

(b) The LB and UB of s in Eq.(6)

(c) The LB and UB of s in Eq.(7)

Figure 2: The bounds of s in Eq.(5), (6), (7)

To draw log-aesthetic space curves, we need to solve simultaneous differential equations, which are the Frenet-Serret formulas. Let $\mathbf{x}(s)$ be a curve and \mathbf{t} , \mathbf{n} , \mathbf{b} be the tangent vector, main normal vector and binormal vector of the curve. We denote a differentiation with respect to s by $'$. Let the curvature and the torsion be $\kappa(= \frac{1}{\rho})$ and $\tau(= \frac{1}{\mu})$, respectively. The curve can be drawn by solving the following simultaneous differential equations

$$\begin{aligned} \mathbf{x}' &= \mathbf{t}(s), & \mathbf{t}' &= \kappa\mathbf{n} \\ \mathbf{n}' &= -\kappa\mathbf{t} + \tau\mathbf{b}, & \mathbf{b}' &= -\tau\mathbf{n} \end{aligned} \quad (8)$$

under the initial conditions at s_0

$$\begin{aligned} \mathbf{x}(s_0) &= \mathbf{x}_0, & \mathbf{t}(s_0) &= \mathbf{t}_0 \\ \mathbf{n}(s_0) &= \mathbf{n}_0, & \mathbf{b}(s_0) &= \mathbf{t}_0 \times \mathbf{n}_0 \end{aligned} \quad (9)$$

Here \mathbf{x}_0 , \mathbf{t}_0 , \mathbf{n}_0 are the initial position, the tangent vector and the main normal vector of the curve at $s = s_0$. From the constraint at the standard form, $\mathbf{x}_0 = [0 \ 0 \ 0]^T$, $\mathbf{t}_0 = [1 \ 0 \ 0]^T$, $\mathbf{n}_0 = [0 \ 1 \ 0]^T$ and $s_0 = 0$.

3. THE FAMILY OF LOG-AESTHETIC SPACE CURVES

To clarify the overall shapes of log-aesthetic curves, we investigate the behavior of tangent and binormal vectors at the lower and the upper bound of s . We define two integrals:

$$\theta(s) = \int_0^s \kappa(u)du \quad \phi(s) = \int_0^s \tau(v)dv \quad (10)$$

For planar curves, $\theta(s)$ is called the tangential angle, which is the angle between the tangent vector and x -axis. For space curves, however, $\theta(s)$ does not have such a geometric meaning since κ and $-\tau$ are the angular velocities of the tangent vector and the binormal vector[3]. Thus if $\theta(s)$ (or $\phi(s)$) is finite at the lower or upper bound, the tangent vector (or the binormal vector) is fixed. If $\theta(s)$ (or $\phi(s)$) is infinite at the lower or upper bound, the tangent vector (or the binormal vector) rotates infinitely toward the bound. Fig.3(a) shows whether $\theta(s)$ of ‘type 1’ and ‘type 2’ curves is infinite or finite depending on α at the bounds of s . Fig.3(b) (or (c)) shows whether $\phi(s)$ of ‘type 1’ (or ‘type 2’) curves is infinite or finite depending on β at the bounds of s .

Fig.4 shows the four cases where the tangent vector and the binormal vector at the bound are either fixed or rotates infinitely. (a) is the case where both the tangent and the binormal vectors are fixed at the (upper) bound of s denoted

	LB	UB
$\alpha < 1$	$-\infty$	Finite
$\alpha = 1$	$-\infty$	∞
$\alpha > 1$	Finite	∞

(a) $\theta(s)$ of 'type 1' or 'type 2' curves

	LB	UB
$\beta < 1$	$-\infty$	Finite
$\beta = 1$	$-\infty$	∞
$\beta > 1$	Finite	∞

(b) $\phi(s)$ of 'type 1' curves

	LB	UB
$\beta < 1$	Finite	∞
$\beta = 1$	$-\infty$	∞
$\beta > 1$	$-\infty$	Finite

(c) $\phi(s)$ of 'type 2' curves

Figure 3: $\theta(s)$ and $\phi(s)$ at the lower bound(LB) or the upper bound(UB)

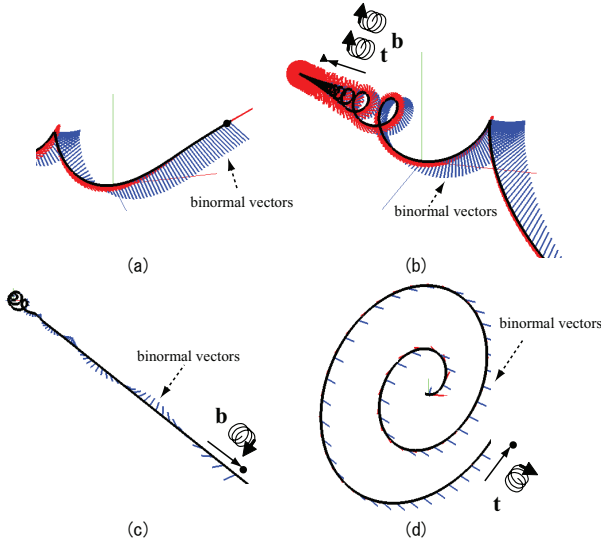


Figure 4: Four cases of log-aesthetic curves

by a black dot. (b) is the case where both the tangent and the binormal vectors rotate infinitely toward the (lower) bound of s . In this case, the curve spirally rotates like a helix. (c) is the case where the tangent vector gets fixed but the binormal vector rotates infinitely toward the (upper) bound of s . The curve gets close to the straight line toward the bound but the binormal vector rotates infinitely. (d) is the case where the binormal vector gets fixed but the tangent vector rotates infinitely toward the (upper) bound of s . In this case, the curve spirally rotates toward the upper bound of s almost in a plane since the binormal vectors of a plane curve are fixed.

To classify log-aesthetic space curves, we also need to know whether the distance to the lower or upper bound of s is finite or infinite from the point at $s = 0$. The bounds of s can be derived from Fig.2. For example, let $\alpha < 0$ and $\beta > 0$ and the curve is a 'type 1' curve. The lower bound is $-\frac{\nu\beta}{\Omega\alpha}$ and the upper bound is $\frac{-1}{\Lambda\alpha}$. In case that the curve is 'type 2' with $\alpha < 0$ and $\beta > 0$, the lower bound is $-\infty$, and the upper bound is the smaller one of $\frac{-1}{\Lambda\alpha}$ and $\frac{\nu\beta}{\Omega\beta}$. If the upper bound is $\frac{-1}{\Lambda\alpha}$, $\rho = \infty$ and $\mu > 0$ at the bound. If

the upper bound is $\frac{\nu\beta}{\Omega\beta}$, $\rho < \infty$ and $\mu = 0$ at the bound. If $\frac{-1}{\Lambda\alpha} = \frac{\nu\beta}{\Omega\beta}$, $\rho = \infty$ and $\mu = 0$ at the bound.

Fig.5 and 6 show the classification of log-aesthetic space curves depending on the arc length toward the point at the lower/upper bound of s , the behavior of tangent and binormal vectors at the lower/upper bound. These characteristics are dependent on α , β , Λ , Ω and ν . Fig.5 is the classification of 'type 1' log-aesthetic curves, whereas Fig.6 is the classification of 'type 2' log-aesthetic curves. In the column θ (or ϕ), $-\infty$ or ∞ means that the tangent (or binormal) vector rotates infinitely toward the point at the lower or upper bound of s . Finite(∞) means that θ (or ϕ) takes a finite value from the constraint of the bound of the radius of torsion (or curvature) on the way to approaching ∞ . Finite(F) means that θ (or ϕ) takes a finite value on the way to approach another finite value. If θ (or ϕ) is finite at the bound, the tangent (or binormal) vector is fixed at the bound. Fig.5 and Fig.6 are important to see the characteristics of log-aesthetic space curves. For example, in 'type 1' curves, the point at $\rho = \infty$ and $\mu = \infty$ with fixed tangent and binormal vectors exists not at infinity only if $\alpha < 0$, $\beta < 0$ and $-\frac{1}{\Lambda\alpha} = -\frac{\nu\beta}{\Omega\beta}$. See the row 'a2' in Fig.5. Other log-aesthetic curves do not have such a point.

Fig.7 and 8 show the overall shapes of log-aesthetic curves in the standard form where Λ , Ω and ν are all 1. Fig.7 shows 'type 1' curves, whereas Fig.8 shows 'type 2' curves. Note that in Fig.7, (a1), (a2), ... correspond to the rows of Fig.5. Similarly in Fig.8, (b1), (b2), ... correspond to the rows of Fig.6. Note also that all the classifications of log-aesthetic curves are not shown in Fig.7 and 8, but they should be easily guessed from Fig.5, 6, 7 and 8.

Log-aesthetic curves depends not only on α and β but also on ν , Λ and Ω . Fig.9 shows log-aesthetic space curves of $\alpha = 0$ ($\Lambda = 1$), $\beta = 0$ ($\Omega = 1$) with various ν s. A large value of ν means that the radius of torsion μ is large at the reference point. Thus the torsion $\tau = 1/\mu$ is small at the reference point. Since $-\tau$ is the angular velocity of binormal vectors, a large value of ν means that binormal vectors get relatively fixed in the increasing direction of s in 'type 1' curves. Setting a large value of ν means that the log-aesthetic space curve gets relatively coplanar in the increasing direction of s .

Fig.10 shows log-aesthetic space curves of $\alpha = 0$, $\beta = 0$ with various Λ s and Ω s. As can be easily found in Eq.(5), $\Lambda = 0$ means $\rho = \text{const}$. Similarly in Eq.(6) and (7), $\Omega = 0$ means $\mu = \text{const}$. Therefore when both Λ and Ω are 0, the radius of curvature ρ and the radius of torsion μ become constants. In such a case, log-aesthetic space curves become helices without depending on α and β . The parameters Λ and Ω can be thought of as the deviations from a helix as they increase from 0. Note that if either Λ or Ω is 0, the characteristics of Fig.5 and 6 do not hold. Taking the limit of ρ (Eq.(5)) as α approaches to $\pm\infty$, ρ becomes a constant. Similarly, taking the limit of μ (Eq.(6) or (7)) as β approaches to $\pm\infty$, μ becomes a constant. Thus log-aesthetic space curves with $\alpha = \pm\infty$ and $\beta = \pm\infty$ also become helices.

No	α	β		At the lower bound of s					At the upper bound of s				
				s	θ	ϕ	ρ	μ	s	θ	ϕ	ρ	μ
a1	$\alpha < 0$	$\beta < 0$	if $(-1/(\Lambda\alpha) > -v^\beta/(\Omega\beta))$	$-\infty$	$-\infty$	$-\infty$	0*	0*	$-v^\beta/(\Omega\beta)$	Finite(F)	Finite	-	∞
a2			if $(-1/(\Lambda\alpha) = -v^\beta/(\Omega\beta))$	$-\infty$	$-\infty$	$-\infty$	0*	0*	$-1/(\Lambda\alpha)$	Finite	Finite	∞	∞
a3			if $(-1/(\Lambda\alpha) < -v^\beta/(\Omega\beta))$	$-\infty$	$-\infty$	$-\infty$	0*	0*	$-1/(\Lambda\alpha)$	Finite	Finite(F)	∞	-
a4		$\beta = 0$	$-\infty$	$-\infty$	$-\infty$	0*	0*	$-1/(\Lambda\alpha)$	Finite	Finite(F)	∞	-	
a5		$0 < \beta < 1$	$-v^\beta/(\Omega\beta)$	Finite($-\infty$)	$-\infty$	-	0*	$-1/(\Lambda\alpha)$	Finite	Finite	∞	-	
a6		$\beta = 1$	$-v^\beta/(\Omega\beta)$	Finite($-\infty$)	$-\infty$	-	0*	$-1/(\Lambda\alpha)$	Finite	Finite(∞)	∞	-	
a7		$\beta > 1$	$-v^\beta/(\Omega\beta)$	Finite($-\infty$)	Finite	-	0	$-1/(\Lambda\alpha)$	Finite	Finite(∞)	∞	-	
a8	$\alpha = 0$	$\beta < 0$	$-\infty$	$-\infty$	$-\infty$	0*	0*	$-v^\beta/(\Omega\beta)$	Finite(F)	Finite	-	∞	
a9		$\beta = 0$	$-\infty$	$-\infty$	$-\infty$	0*	0*	∞	Finite	Finite	∞ *	∞ *	
a10		$0 < \beta < 1$	$-v^\beta/(\Omega\beta)$	Finite($-\infty$)	$-\infty$	-	0*	∞	Finite	Finite	∞ *	∞ *	
a11		$\beta = 1$	$-v^\beta/(\Omega\beta)$	Finite($-\infty$)	$-\infty$	-	0*	∞	Finite	∞	∞ *	∞ *	
a12		$\beta > 1$	$-v^\beta/(\Omega\beta)$	Finite($-\infty$)	Finite	-	0	∞	Finite	∞	∞ *	∞ *	
a13		$\beta < 0$	$-1/(\Lambda\alpha)$	$-\infty$	Finite($-\infty$)	0*	-	$-v^\beta/(\Omega\beta)$	Finite(F)	Finite	-	∞	
a14	$\beta = 0$	$-1/(\Lambda\alpha)$	$-\infty$	Finite($-\infty$)	0*	-	∞	Finite	Finite	∞ *	∞ *		
a15	$0 < \alpha < 1$	$0 < \beta < 1$	if $(-1/(\Lambda\alpha) > -v^\beta/(\Omega\beta))$	$-1/(\Lambda\alpha)$	$-\infty$	Finite($-\infty$)	0*	-	∞	Finite	Finite	∞ *	∞ *
a16			if $(-1/(\Lambda\alpha) = -v^\beta/(\Omega\beta))$	$-1/(\Lambda\alpha)$	$-\infty$	$-\infty$	0*	0*	∞	Finite	Finite	∞ *	∞ *
a17			if $(-1/(\Lambda\alpha) < -v^\beta/(\Omega\beta))$	$-v^\beta/(\Omega\beta)$	Finite($-\infty$)	$-\infty$	-	0*	∞	Finite	Finite	∞ *	∞ *
a18		$\beta = 1$	if $(-1/(\Lambda\alpha) > -v^\beta/(\Omega\beta))$	$-1/(\Lambda\alpha)$	$-\infty$	Finite($-\infty$)	0*	-	∞	Finite	∞	∞ *	∞ *
a19			if $(-1/(\Lambda\alpha) = -v^\beta/(\Omega\beta))$	$-1/(\Lambda\alpha)$	$-\infty$	$-\infty$	0*	0*	∞	Finite	∞	∞ *	∞ *
a20			if $(-1/(\Lambda\alpha) < -v^\beta/(\Omega\beta))$	$-v^\beta/(\Omega\beta)$	Finite($-\infty$)	$-\infty$	-	0*	∞	Finite	∞	∞ *	∞ *
a21		$\beta > 1$	if $(-1/(\Lambda\alpha) > -v^\beta/(\Omega\beta))$	$-1/(\Lambda\alpha)$	$-\infty$	Finite(F)	0*	-	∞	Finite	∞	∞ *	∞ *
a22			if $(-1/(\Lambda\alpha) = -v^\beta/(\Omega\beta))$	$-1/(\Lambda\alpha)$	$-\infty$	Finite	0*	0	∞	Finite	∞	∞ *	∞ *
a23			if $(-1/(\Lambda\alpha) < -v^\beta/(\Omega\beta))$	$-v^\beta/(\Omega\beta)$	Finite($-\infty$)	Finite	-	0	∞	Finite	∞	∞ *	∞ *
a24	$\alpha = 1$	$\beta < 0$	$-1/(\Lambda\alpha)$	$-\infty$	Finite($-\infty$)	0*	-	$-v^\beta/(\Omega\beta)$	Finite(F)	Finite	-	∞	
a25		$\beta = 0$	$-1/(\Lambda\alpha)$	$-\infty$	Finite($-\infty$)	0*	-	∞	∞	Finite	∞ *	∞ *	
a26		$0 < \beta < 1$	if $(-1/(\Lambda\alpha) > -v^\beta/(\Omega\beta))$	$-1/(\Lambda\alpha)$	$-\infty$	Finite($-\infty$)	0*	-	∞	∞	∞ *	∞ *	
a27			if $(-1/(\Lambda\alpha) = -v^\beta/(\Omega\beta))$	$-1/(\Lambda\alpha)$	$-\infty$	$-\infty$	0*	0*	∞	∞	Finite	∞ *	∞ *
a28			if $(-1/(\Lambda\alpha) < -v^\beta/(\Omega\beta))$	$-v^\beta/(\Omega\beta)$	Finite($-\infty$)	$-\infty$	-	0*	∞	∞	Finite	∞ *	∞ *
a29		$\beta = 1$	if $(-1/(\Lambda\alpha) > -v^\beta/(\Omega\beta))$	$-1/(\Lambda\alpha)$	$-\infty$	Finite($-\infty$)	0*	-	∞	∞	∞ *	∞ *	
a30			if $(-1/(\Lambda\alpha) = -v^\beta/(\Omega\beta))$	$-1/(\Lambda\alpha)$	$-\infty$	$-\infty$	0*	0*	∞	∞	∞ *	∞ *	
a31			if $(-1/(\Lambda\alpha) < -v^\beta/(\Omega\beta))$	$-v^\beta/(\Omega\beta)$	Finite($-\infty$)	$-\infty$	-	0*	∞	∞	∞ *	∞ *	
a32		$\beta > 1$	if $(-1/(\Lambda\alpha) > -v^\beta/(\Omega\beta))$	$-1/(\Lambda\alpha)$	$-\infty$	Finite(F)	0*	-	∞	∞	∞ *	∞ *	
a33			if $(-1/(\Lambda\alpha) = -v^\beta/(\Omega\beta))$	$-1/(\Lambda\alpha)$	$-\infty$	Finite	0*	0	∞	∞	∞ *	∞ *	
a34			if $(-1/(\Lambda\alpha) < -v^\beta/(\Omega\beta))$	$-v^\beta/(\Omega\beta)$	Finite($-\infty$)	Finite	-	0	∞	∞	∞ *	∞ *	
a35		$\alpha > 1$	$\beta < 0$	$-1/(\Lambda\alpha)$	Finite	Finite($-\infty$)	0	-	$-v^\beta/(\Omega\beta)$	Finite(F)	Finite	-	∞
a36	$\beta = 0$		$-1/(\Lambda\alpha)$	Finite	Finite($-\infty$)	0	-	∞	∞	Finite	∞ *	∞ *	
a37	$0 < \beta < 1$		if $(-1/(\Lambda\alpha) > -v^\beta/(\Omega\beta))$	$-1/(\Lambda\alpha)$	Finite	Finite($-\infty$)	0	-	∞	∞	Finite	∞ *	∞ *
a38			if $(-1/(\Lambda\alpha) = -v^\beta/(\Omega\beta))$	$-1/(\Lambda\alpha)$	Finite	$-\infty$	0	0*	∞	∞	Finite	∞ *	∞ *
a39			if $(-1/(\Lambda\alpha) < -v^\beta/(\Omega\beta))$	$-v^\beta/(\Omega\beta)$	Finite(F)	$-\infty$	-	0*	∞	∞	Finite	∞ *	∞ *
a40	$\beta = 1$		if $(-1/(\Lambda\alpha) > -v^\beta/(\Omega\beta))$	$-1/(\Lambda\alpha)$	Finite	Finite($-\infty$)	0	-	∞	∞	∞ *	∞ *	
a41			if $(-1/(\Lambda\alpha) = -v^\beta/(\Omega\beta))$	$-1/(\Lambda\alpha)$	Finite	$-\infty$	0	0*	∞	∞	∞ *	∞ *	
a42			if $(-1/(\Lambda\alpha) < -v^\beta/(\Omega\beta))$	$-v^\beta/(\Omega\beta)$	Finite(F)	$-\infty$	-	0*	∞	∞	∞ *	∞ *	
a43	$\beta > 1$		if $(-1/(\Lambda\alpha) > -v^\beta/(\Omega\beta))$	$-1/(\Lambda\alpha)$	Finite	Finite(F)	0	-	∞	∞	∞ *	∞ *	
a44			if $(-1/(\Lambda\alpha) = -v^\beta/(\Omega\beta))$	$-1/(\Lambda\alpha)$	Finite	Finite	0	0	∞	∞	∞ *	∞ *	
a45			if $(-1/(\Lambda\alpha) < -v^\beta/(\Omega\beta))$	$-v^\beta/(\Omega\beta)$	Finite(F)	Finite	-	0	∞	∞	∞ *	∞ *	

In θ and ϕ columns,

'Finite(∞)' means that θ (or ϕ) approaches to a finite value on the way to approach to ∞ .

'Finite(F)' means that θ (or ϕ) approaches to a finite value on the way to approach to another finite value.

In ρ and μ columns,

'**' indicates that either the arc length is infinite or the tangential or binormal direction is not determined at the bound.

If s is infinite at the bound, the arc length is infinite to the bound.

If θ (or ϕ) is infinite at the bound, the tangential (or binormal) vector rotates infinitely toward the bound.

Figure 5: Classification of 'type 1' log-aesthetic space curves

No	α	β	At the lower bound of s					At the upper bound of s						
			s	θ	ϕ	ρ	μ	s	θ	ϕ	ρ	μ		
b1	$\alpha < 0$	$\beta < 0$	$v^\beta/(\Omega\beta)$	Finite(- ∞)	Finite	-	∞	$-1/(\Lambda\alpha)$	Finite	Finite(∞)	∞	-		
b2		$\beta = 0$	$-\infty$	$-\infty$	Finite	0*	$\infty*$	$-1/(\Lambda\alpha)$	Finite	Finite(∞)	∞	-		
b3		$0 < \beta < 1$	if $(-1/(\Lambda\alpha) < v^\beta/(\Omega\beta))$	$-\infty$	$-\infty$	Finite	0*	$\infty*$	$-1/(\Lambda\alpha)$	Finite	Finite(∞)	∞	-	
b4			if $(-1/(\Lambda\alpha) = v^\beta/(\Omega\beta))$	$-\infty$	$-\infty$	Finite	0*	$\infty*$	$-1/(\Lambda\alpha)$	Finite	∞	∞	0*	
b5			if $(-1/(\Lambda\alpha) > v^\beta/(\Omega\beta))$	$-\infty$	$-\infty$	Finite	0*	$\infty*$	$v^\beta/(\Omega\beta)$	Finite(F)	∞	-	0*	
b6		$\beta = 1$	if $(-1/(\Lambda\alpha) < v^\beta/(\Omega\beta))$	$-\infty$	$-\infty$	$-\infty$	0*	$\infty*$	$-1/(\Lambda\alpha)$	Finite	Finite(∞)	∞	-	
b7			if $(-1/(\Lambda\alpha) = v^\beta/(\Omega\beta))$	$-\infty$	$-\infty$	$-\infty$	0*	$\infty*$	$-1/(\Lambda\alpha)$	Finite	∞	∞	0*	
b8			if $(-1/(\Lambda\alpha) > v^\beta/(\Omega\beta))$	$-\infty$	$-\infty$	$-\infty$	0*	$\infty*$	$v^\beta/(\Omega\beta)$	Finite(F)	∞	-	0*	
b9		$\beta > 1$	if $(-1/(\Lambda\alpha) < v^\beta/(\Omega\beta))$	$-\infty$	$-\infty$	$-\infty$	0*	$\infty*$	$-1/(\Lambda\alpha)$	Finite	Finite(F)	∞	-	
b10			if $(-1/(\Lambda\alpha) = v^\beta/(\Omega\beta))$	$-\infty$	$-\infty$	$-\infty$	0*	$\infty*$	$-1/(\Lambda\alpha)$	Finite	Finite	∞	0	
b11			if $(-1/(\Lambda\alpha) > v^\beta/(\Omega\beta))$	$-\infty$	$-\infty$	$-\infty$	0*	$\infty*$	$v^\beta/(\Omega\beta)$	Finite(F)	Finite	-	0	
b12	$\alpha = 0$	$\beta < 0$	$v^\beta/(\Omega\beta)$	Finite(- ∞)	Finite	-	∞	∞	Finite	∞	-	0*		
b13		$\beta = 0$	$-\infty$	$-\infty$	Finite	0*	$\infty*$	∞	Finite	∞	$\infty*$	0*		
b14		$0 < \beta < 1$	$-\infty$	$-\infty$	Finite	0*	$\infty*$	$v^\beta/(\Omega\beta)$	Finite(F)	∞	-	0*		
b15		$\beta = 1$	$-\infty$	$-\infty$	$-\infty$	0*	$\infty*$	$v^\beta/(\Omega\beta)$	Finite(F)	∞	-	0*		
b16		$\beta > 1$	$-\infty$	$-\infty$	$-\infty$	0*	$\infty*$	$v^\beta/(\Omega\beta)$	Finite(F)	Finite	-	0		
b17		$0 < \alpha < 1$	$\beta < 0$	if $(-1/(\Lambda\alpha) < v^\beta/(\Omega\beta))$	$v^\beta/(\Omega\beta)$	Finite(- ∞)	Finite	-	∞	∞	∞	$\infty*$	0*	
b18	if $(-1/(\Lambda\alpha) = v^\beta/(\Omega\beta))$			$-1/(\Lambda\alpha)$	$-\infty$	Finite	0*	$\infty*$	∞	Finite	∞	$\infty*$	0*	
b19	if $(-1/(\Lambda\alpha) > v^\beta/(\Omega\beta))$			$-1/(\Lambda\alpha)$	$-\infty$	Finite(F)	0*	-	∞	Finite	∞	$\infty*$	0*	
b20	$\beta = 0$		$-1/(\Lambda\alpha)$	$-\infty$	Finite(F)	0*	-	∞	Finite	∞	$\infty*$	0*		
b21	$0 < \beta < 1$		$-1/(\Lambda\alpha)$	$-\infty$	Finite(F)	0*	-	$v^\beta/(\Omega\beta)$	Finite(F)	∞	-	0*		
b22	$\beta = 1$		$-1/(\Lambda\alpha)$	$-\infty$	Finite(- ∞)	0*	-	$v^\beta/(\Omega\beta)$	Finite(F)	∞	-	0*		
b23	$\beta > 1$		$-1/(\Lambda\alpha)$	$-\infty$	Finite(- ∞)	0*	-	$v^\beta/(\Omega\beta)$	Finite(F)	Finite	-	0		
b24	$\alpha = 1$		$\beta < 0$	if $(-1/(\Lambda\alpha) < v^\beta/(\Omega\beta))$	$v^\beta/(\Omega\beta)$	Finite(- ∞)	Finite	-	∞	∞	∞	$\infty*$	0*	
b25				if $(-1/(\Lambda\alpha) = v^\beta/(\Omega\beta))$	$-1/(\Lambda\alpha)$	$-\infty$	Finite	0*	∞	∞	∞	∞	$\infty*$	0*
b26				if $(-1/(\Lambda\alpha) > v^\beta/(\Omega\beta))$	$-1/(\Lambda\alpha)$	$-\infty$	Finite(F)	0*	-	∞	∞	∞	$\infty*$	0*
b27		$\beta = 0$	$-1/(\Lambda\alpha)$	$-\infty$	Finite(F)	0*	-	∞	∞	∞	$\infty*$	0*		
b28		$0 < \beta < 1$	$-1/(\Lambda\alpha)$	$-\infty$	Finite(F)	0*	-	$v^\beta/(\Omega\beta)$	Finite(∞)	∞	-	0*		
b29		$\beta = 1$	$-1/(\Lambda\alpha)$	$-\infty$	Finite(- ∞)	0*	-	$v^\beta/(\Omega\beta)$	Finite(∞)	∞	-	0*		
b30		$\beta > 1$	$-1/(\Lambda\alpha)$	$-\infty$	Finite(- ∞)	0*	-	$v^\beta/(\Omega\beta)$	Finite(∞)	Finite	-	0		
b31		$\alpha > 1$	$\beta < 0$	if $(-1/(\Lambda\alpha) < v^\beta/(\Omega\beta))$	$v^\beta/(\Omega\beta)$	Finite(F)	Finite	-	∞	∞	∞	$\infty*$	0*	
b32				if $(-1/(\Lambda\alpha) = v^\beta/(\Omega\beta))$	$-1/(\Lambda\alpha)$	Finite	Finite	0	∞	∞	∞	∞	$\infty*$	0*
b33				if $(-1/(\Lambda\alpha) > v^\beta/(\Omega\beta))$	$-1/(\Lambda\alpha)$	Finite	Finite(F)	0	-	∞	∞	∞	$\infty*$	0*
b34	$\beta = 0$		$-1/(\Lambda\alpha)$	Finite	Finite(F)	0	-	∞	∞	∞	$\infty*$	0*		
b35	$0 < \beta < 1$		$-1/(\Lambda\alpha)$	Finite	Finite(F)	0	-	$v^\beta/(\Omega\beta)$	Finite(∞)	∞	-	0*		
b36	$\beta = 1$		$-1/(\Lambda\alpha)$	Finite	Finite(- ∞)	0	-	$v^\beta/(\Omega\beta)$	Finite(∞)	∞	-	0*		
b37	$\beta > 1$		$-1/(\Lambda\alpha)$	Finite	Finite(- ∞)	0	-	$v^\beta/(\Omega\beta)$	Finite(∞)	Finite	-	0		

In θ and ϕ columns,

'Finite(∞)' means that θ (or ϕ) approaches to a finite value on the way to approach to ∞ .

'Finite(F)' means that θ (or ϕ) approaches to a finite value on the way to approach to another finite value.

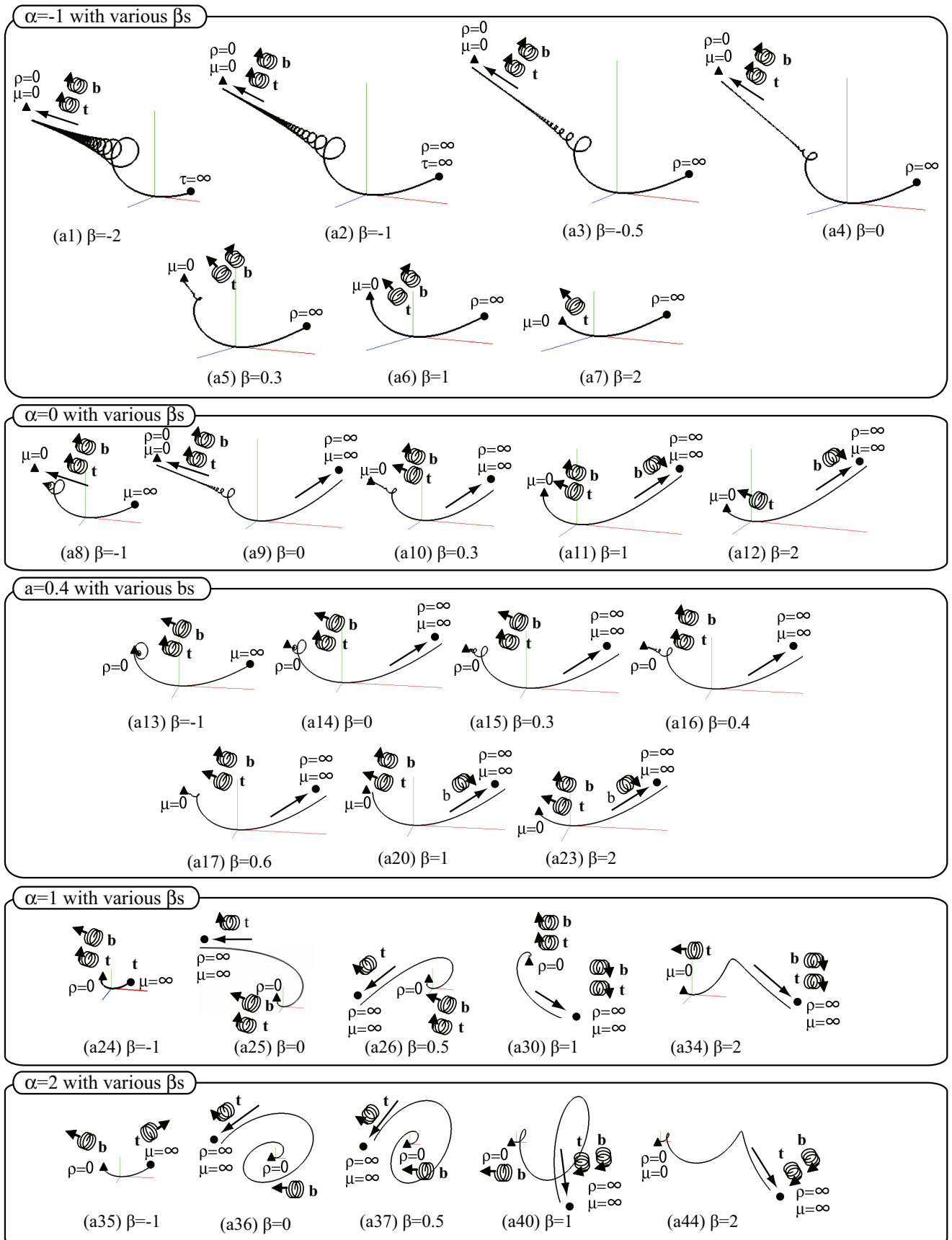
In ρ and μ columns,

'*' indicates that either the arc length is infinite or the tangential or binormal direction is not determined at the bound.

If s is infinite at the bound, the arc length is infinite to the bound.

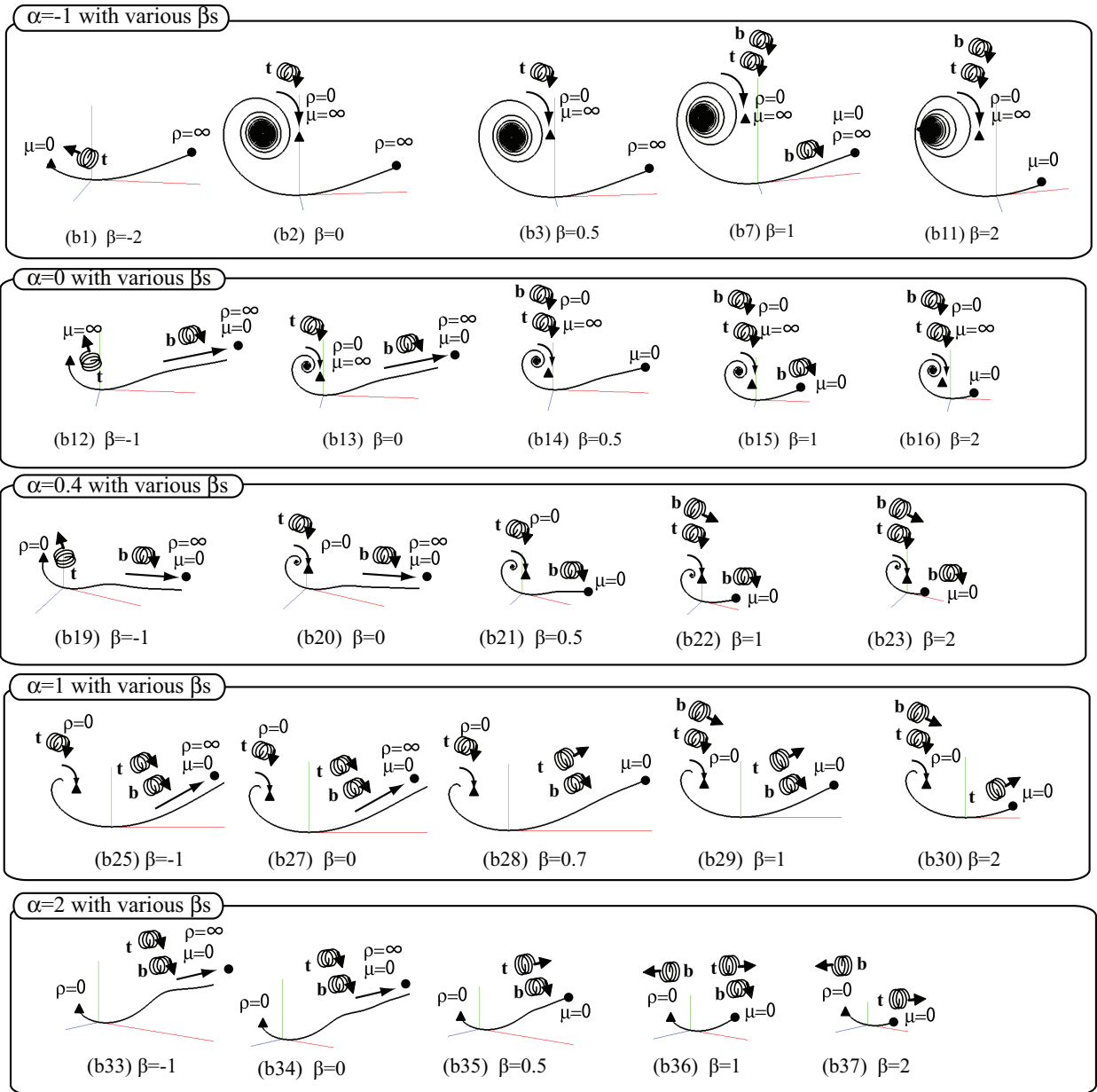
If θ (or ϕ) is infinite at the bound, the tangential (or binormal) vector rotates infinitely toward the bound.

Figure 6: Classification of 'type 2' log-aesthetic space curves



● The point of the upper bound of s . ▲ The point of the lower bound of s . ● ← The distance to the limit point is infinite.
 ↗ (●) The binormal or tangent vector rotates infinitely toward the upper or lower bound of s . ● ← The distance to the limit point is finite.
 ← (●) The direction of the binormal or tangent vector is rotationally fixed at the lower or upper bound of s . t: tangent vector
 * When not indicated, the tangent or binormal vector is determined at the upper or lower bound of s . b: binormal vector

Figure 7: 'type 1' log-aesthetic space curves ($\Lambda = 1, \Omega = 1, \nu = 1$)



● The point of the upper bound of s . ▲ The point of the lower bound of s . ● ← The distance to the limit point is infinite.
 ▲ ⊙ The binormal or tangent vector rotates infinitely toward the upper or lower bound of s . ● ← The distance to the limit point is finite.
 ● ⊙ The direction of the binormal or tangent vector is rotationally fixed at the lower or upper bound of s . t: tangent vector
 * When not indicated, the tangent or binormal vector is determined at the upper or lower bound of s . b: binormal vector

Figure 8: 'type 2' log-aesthetic space curves ($\Lambda = 1, \Omega = 1, \nu = 1$)

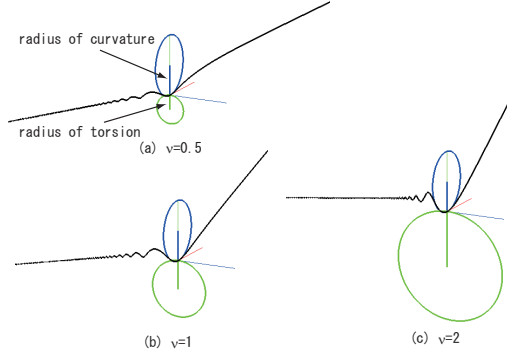


Figure 9: Log-aesthetic space curves of $\alpha = 0(\Lambda = 1), \beta = 0(\Omega = 1)$ with various ν s.

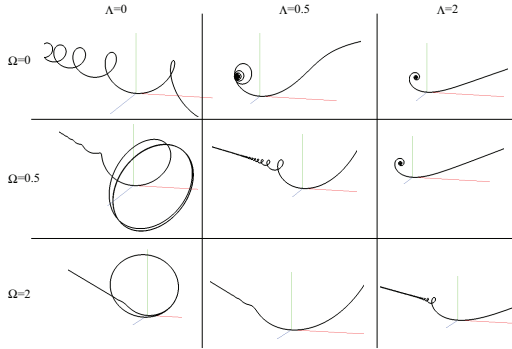


Figure 10: Log-aesthetic space curves of $\alpha = 0$ and $\beta = 0$ with various Λ s and Ω s.

4. LOG-AESTHETIC SPACE CURVE SEGMENTS

We present a method for drawing a log-aesthetic space curve segment by specifying two endpoints, their tangents, the slopes of the LCG and LTG, α, β , the torsion parameter Ω and the ‘type’. Ω is exactly the same as it appears in Eq.(6) or Eq.(7). The reason why we specify Ω will be described shortly. In the discussion below, we assume that α, β and the ‘type’ of the curve segment are specified except when explicitly denoted. The idea for finding a curve segment that satisfies the endpoint constraints is searched for from the overall shape in the standard form and then a similarity transformation to the points on the curve segment is performed, which implies that log-aesthetic curve segments are invariant under similarity transformation. The generation algorithm, however, is not a simple extension of [18] because of the tangential angle problem and the problems of the additional degree of freedom.

We are given the four points $\mathbf{P}_0, \mathbf{P}_1, \mathbf{P}_2$ and \mathbf{P}_3 . The two endpoints are \mathbf{P}_0 and \mathbf{P}_3 , and their tangents are $\mathbf{v}_0 = \frac{\mathbf{P}_1 - \mathbf{P}_0}{|\mathbf{P}_1 - \mathbf{P}_0|}$ and $\mathbf{v}_1 = \frac{\mathbf{P}_3 - \mathbf{P}_2}{|\mathbf{P}_3 - \mathbf{P}_2|}$, respectively. Since log-aesthetic curve segments are invariant under similarity transformation, we position the four points in the following manner. We set $\mathbf{P}_0 = [-1 \ 0 \ 0]^T$, $\mathbf{P}_3 = [1 \ 0 \ 0]^T$ and $|\mathbf{P}_1 - \mathbf{P}_0| = 1$. \mathbf{P}_1 is on the xy plane and the angle between $\mathbf{P}_1 - \mathbf{P}_0$ and

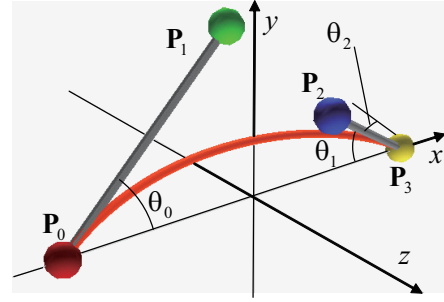


Figure 11: Four points characterized by θ_0, θ_1 and θ_2 .

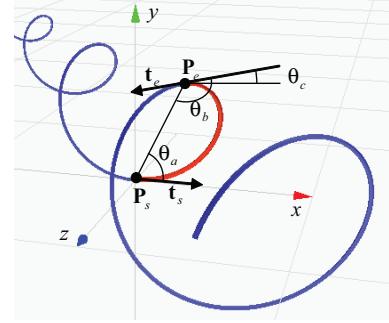


Figure 12: Two endpoints and their tangents of a curve segment in the overall shape

$[1 \ 0 \ 0]^T$ is θ_0 . \mathbf{P}_2 is positioned such that $\mathbf{P}_2 - \mathbf{P}_3$ is a vector $[-1 \ 0 \ 0]^T$ which is rotated θ_1 about z axis and then rotated θ_2 about x axis. See Fig.11. From any valid four points, we can compute the three angles θ_0, θ_1 and θ_2 . Since our definition of log-aesthetic curves does not include plane curves ($\nu = \infty$ for planar curves), θ_2 should not be 0.

Suppose that the parameters Λ, Ω, ν for drawing a curve segment in the standard form as well as the arc length of the segment $s_1 (> 0)$ are known. We can draw a log-aesthetic curve segment in the standard form from the point (\mathbf{P}_s) at $s = 0$ to the point (\mathbf{P}_e) at $s = s_1$. Let \mathbf{t}_s and \mathbf{t}_e be the tangents at \mathbf{P}_s and \mathbf{P}_e , respectively. See Fig.12. From these endpoints and their tangents, we compute three angles θ_a, θ_b and θ_c : θ_a is the angle formed by \mathbf{t}_s and $\mathbf{P}_e - \mathbf{P}_s$. θ_b is the angle formed by $-\mathbf{t}_e$ and $\mathbf{P}_s - \mathbf{P}_e$. θ_c is the angle formed by \mathbf{t}_e and the plane that goes through $\mathbf{P}_s, \mathbf{P}_s + \mathbf{t}_e$ and \mathbf{P}_e . The problem for finding a curve segment that satisfies the endpoint constraint is to find Λ, Ω, ν and s_1 such that $\theta_a = \theta_0, \theta_b = \theta_1$ and $\theta_c = \theta_2$.

For various log-aesthetic space curves, we have compared the angle θ_a with θ_b and found that θ_a is greater than θ_b in most cases. Very rarely, θ_b gets greater than θ_a . In case of log-aesthetic planar curves where $\theta_c = 0$ and the curve exists in xy plane, θ_a is always larger than or equal to θ_b . However, the space curves have torsion and θ_b may get larger than θ_a . Since $\theta_a > \theta_b$ in most cases, we assume that $\theta_0 \geq \theta_1$. If this does not hold, we just swap the coordinates and tangents of two endpoints. By assuming $\theta_0 \geq \theta_1$, the cases where curve segments are found for various θ_0, θ_1 , and θ_2 increase

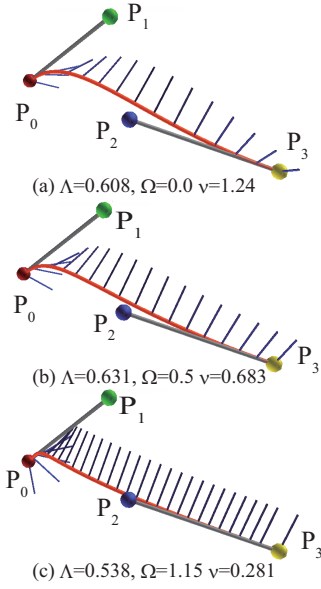


Figure 13: Type 1 log-aesthetic curve segments($\alpha = 0, \beta = 0$) with the same endpoint constraints. Binormals are shown.

greatly.

As shown in Fig.13, we found that three parameters, Λ , Ω and ν , are not uniquely decided when two endpoints and their tangents are specified. We also found that if one of the parameters is specified, other two parameters are decided. Thus we need to specify one of the three parameters. Among three parameters, we found that only Ω can be modified from 0 to a certain positive value Ω_{\max} , which depends on α , β and the endpoint constraints. Moreover, $\Omega = 0$ means that the torsion is a constant without depending on β . Instead of specifying Ω , it is possible to specify binormal vectors at two endpoints. However, by changing the value of Ω , we found that the region of the binormal vectors in which a curve segment can be drawn is very restricted and not easy to predictable. Thus we decided to specify Ω in addition to two endpoints and their tangents. This is our answer to the problem (2a) given in Section 1.

For generating a curve segment that satisfies the endpoint constraints, we first generate a curve segment such that (a) the positional and tangential constraints at the start point and the positional constraint at the end point are satisfied. Then (b) the tangential constraint at the end point is satisfied. For a curve segment to satisfy the condition (a), we propose a cone-intersection method. The condition (b) is satisfied by a minimization.

We consider generating a curve segment that satisfies the condition (a). We translate the four points $\mathbf{P}_0, \dots, \mathbf{P}_3$ such that \mathbf{P}_0 goes to the origin, rotate them so that \mathbf{P}_1 is at $[1 \ 0 \ 0]^T$ and \mathbf{P}_3 exists on the xy plane. We call the transformed points, $\mathbf{P}_a, \mathbf{P}_b, \mathbf{P}_c$ and \mathbf{P}_d , respectively. See Fig.14. Now \mathbf{P}_a is at the origin and the curve's tangent vector at \mathbf{P}_a is $[1 \ 0 \ 0]^T$. The position \mathbf{P}_a and its tangent agree with the position and its tangent of all the log-aesthetic curves

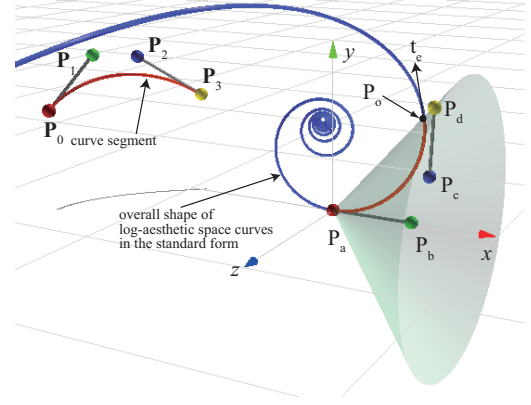


Figure 14: Transformed points, the cone and the overall shape

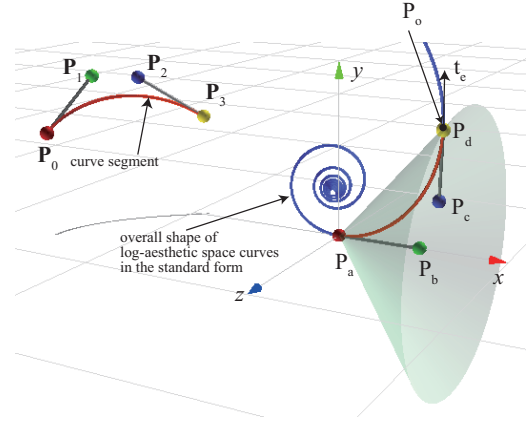


Figure 15: The overall shape of Fig.14 is rotated and scaled.

in the standard form with the start point at $s = 0$ and the endpoint at $s = s_1$, which is not known yet.

By rotating 2π a half line that starts from the origin(\mathbf{P}_a) and goes through \mathbf{P}_d about the x -axis, we can construct a cone as shown in Fig.14. Suppose that a curve segment in the standard form intersects the cone at the point \mathbf{P}_o . Let the unit tangent vector of the curve segment at \mathbf{P}_o be \mathbf{t}_e , which we will use later. By rotating the curve segment about x axis such that \mathbf{P}_o exists in the xy plane and then scaling the curve segment by $\frac{|\mathbf{P}_d|}{|\mathbf{P}_o|}$, the endpoint of the curve coincides with \mathbf{P}_d . Note that if $\theta_2 = \pm\pi/2$, the segment $\mathbf{P}_c\mathbf{P}_d$ exists on the tangent plane of the cone at \mathbf{P}_d . Thus, if $|\theta_2| > \pi/2$, we need to find the second intersection point of the curve with the cone. See Fig.16. In Fig.16, the overall shape is rotated and scaled such that the endpoint of the curve segment coincides with \mathbf{P}_d . Thus if a log-aesthetic curve in the standard form intersects the cone, the condition (a) is satisfied. This is our answer to the problem (1). Let $\mathbf{t}_f = \frac{\mathbf{P}_d - \mathbf{P}_c}{|\mathbf{P}_d - \mathbf{P}_c|}$. To satisfy the condition (b), we need to find Λ and ν such that $\mathbf{t}_e = \mathbf{t}_f$. We perform a minimization such that

$$f(\Lambda, \nu) = |\mathbf{t}_e \cdot \mathbf{t}_f - 1| \quad (11)$$

becomes 0. Note that if the signs of z coordinates of \mathbf{t}_f and

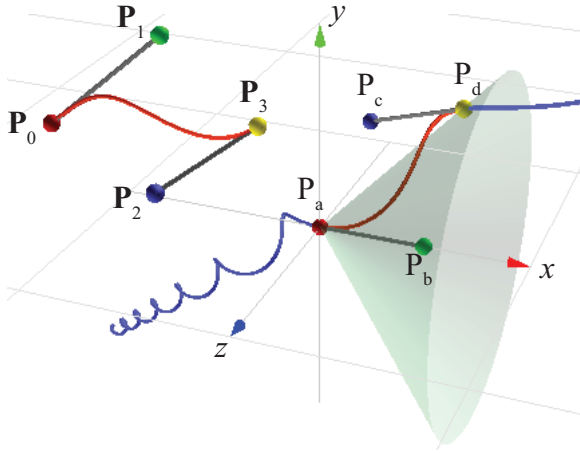


Figure 16: The case of $\theta_2 > \pi/2$

t_e are different, the z coordinates of t_e is reversed. In this case, we also need to reverse all the z coordinates of the points on the curve segment.

When minimizing Eq.(11), we have to be careful that $\Lambda \geq 0$ and $\nu > 0$. We also have to be careful that the log-aesthetic curve may have its upper bound and the curve reaches the upper bound before it intersects the cone. In such a case, Eq.(11) is not defined.

We use the following approach to modify Nelder and Mead's downhill simplex method [15] such that the method works even when $f(\Lambda, \nu)$ may not be defined, and Λ and ν can be arbitrarily small but never be negative. In the downhill simplex method of two parameters, the three simplex points are moved like an amoeba so that they get closer to the minimum. See Fig.17 for the four kinds of steps. In each of the four steps, if $f(\Lambda, \nu)$ is not defined at the new simplex point moved, we move the simplex point back toward the original point until $f(\Lambda, \nu)$ is defined and the three simplex points are confirmed to be linearly independent. Λ and ν may become negative only when a reflection step is performed. Suppose that Λ became negative as shown in Fig.18. In this case the Λ of the new point is set to $1/n$ ($n=10$ in our implementation) of the Λ s of p_0 and p_1 .

Each initial point is chosen such that Eq.(11) is defined and they are not collinear. Without depending on α and β , every log-aesthetic curve becomes a helix when $\Lambda = 0$ and $\Omega = 0$. Since a helix always intersects the cone constructed from the four points, Eq.(11) is defined when Λ and Ω are near 0 and ν is moved such that the upper bound gets larger. For a large value of Ω , the initial simplex points are not found and therefore the curve segment is not found. In our implementation, we found that the modified downhill simplex method works fairly well. Now we have partially answered to the problem (2b).

Using the above algorithm, we can find a curve segment that satisfies the endpoint constraints. However, there might be a case where an undesirable curve segment, such as the one shown in Fig.19(a), is computed. To avoid such a curve segment, we compute the sum of the changes of tangent vectors

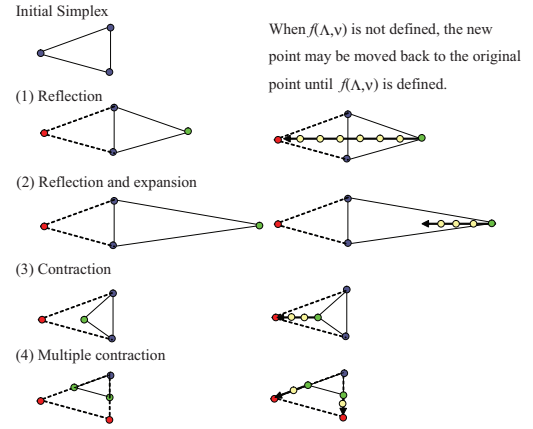


Figure 17: Modified downhill simplex method for dealing with the case when $f(\Lambda, \nu)$ is not defined.

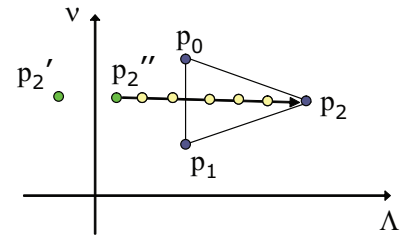


Figure 18: Modified downhill simplex method so that Λ, ν can be arbitrarily small but never be negative.

and the sum of the changes of binormal vectors. If either of the sums is greater than 2π , we set $f(\Lambda, \nu)$ undefined. This guarantees that the tangent vectors and binormal vectors of the curve segment never rotate more than 2π . Fig.19(b) shows the desirable curve segment with the same endpoint constraints.

Fig. 20 shows log-aesthetic space curve segments generated by the proposed method. To help understand the 3D shape of the curve segment, the shadows are also shown. The accuracy of the curve segment depends of Δ_s for solving Eq.(8) and the epsilon ϵ_f for Eq.(11). In our implementation, the generation time for a curve segment is around 10ms on a Core2 Quad 2.4GHz processor for $\Delta_s = 0.005$ and $\epsilon = 1 \times 10^{-5}$. Therefore, we can interactively control a curve segment, which answers to the problem (2b).

The position of the four points (thus θ_0, θ_1 and θ_2), α, β and Ω dictate whether a curve segment is drawn or not. As $|\alpha|, |\beta|$, or Ω gets larger, the cases where curve segments are drawn with various θ_0, θ_1 and θ_2 decrease. We use four points to control a log-aesthetic curve segment. Thus, one may wonder if the convex hull property or the variation diminishing property holds. However, what we really use to control a segment are two endpoints and their tangents. Thus, these properties cannot be defined. The uniqueness of the generated curve segment with a specified condition is not proved. However, there is no visible oscillation in generating curve segments, so it seems to be unique.

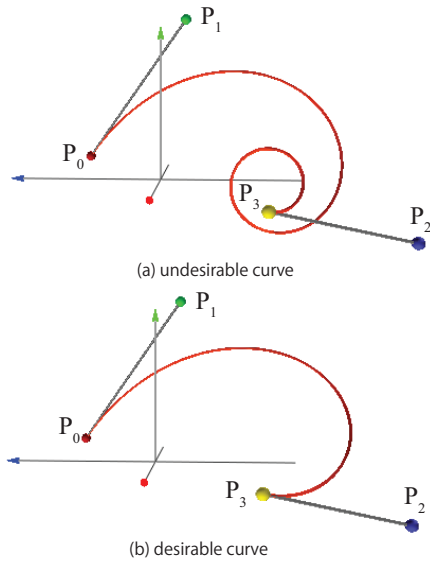


Figure 19: Undesirable and desirable curve segments

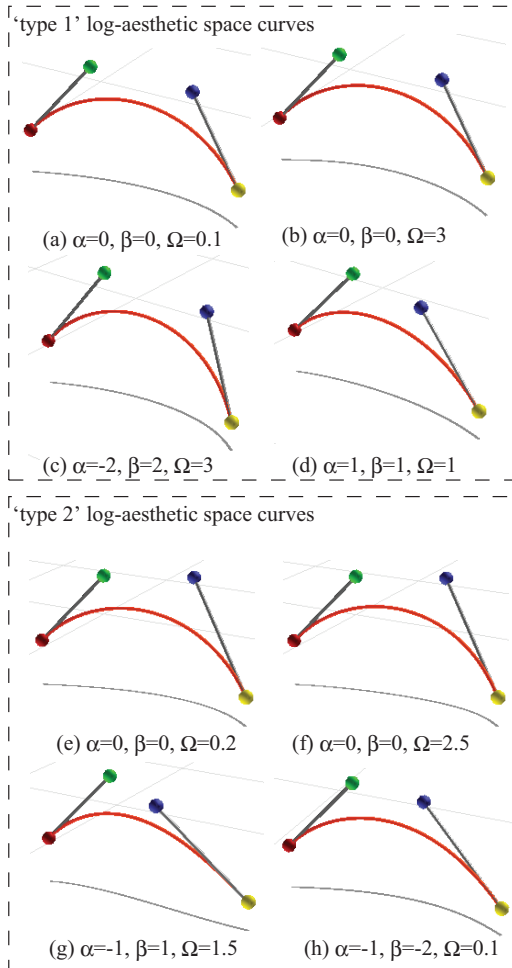


Figure 20: Log-aesthetic space curve segments

5. CONCLUSIONS

In this paper, we have defined and classified log-aesthetic space curves, which are curves whose logarithmic curvature and torsion graphs are both linear. We have also proposed a method for interactively controlling a log-aesthetic space curve segment. The classification is based on the arc length toward the point at 0 or infinite curvature or torsion, and the behavior of the tangent and binormal vectors toward such points. The classification is important to see, for example, which curve has a point at $\rho = \infty$ and $\mu = \infty$ not at infinity. A log-aesthetic space curve segment is controlled by specifying two endpoints, their tangents, the slopes of logarithmic curvature and torsion graphs, α and β , and the torsion parameter Ω . Log-aesthetic space curve segments can be controlled fully interactively.

Future work includes the approximation of log-aesthetic space curves by free-form curves, such as NURBS or Bézier curves, and the generation of aesthetic surfaces using log-aesthetic space curves. For connecting segments, the method of [12] may be extended for space curves.

6. REFERENCES

- [1] J. A. Adams. The intrinsic method for curve definition. *Computer Aided Design*, 7(4):243–249, 1975.
- [2] M. P. D. Carmo. *Differential Geometry of Curves and Surfaces*. Prentice-Hall, 1976.
- [3] G. Farin. *Curves and Surfaces for CAGD Fifth Edition*. Morgan Kaufmann Publishers, 2002.
- [4] G. Farin. Class A Bézier curves. *Computer-Aided Geometric Design*, 23(7):573–581, 2006.
- [5] R. T. Farouki, H. P. Moon, and B. Ravani. Algorithms for mikowski products and implicitly-defined complex sets. *Advances in Computational Mathematics*, 13(3):199–229, 2000.
- [6] W. H. Frey and D. A. Field. Designing bézier conic segments with monotone curvature. *Computer-Aided Geometric Design*, 17(6):457–483, 2000.
- [7] R. Fukuda, N. Yoshida, and T. Saito. Interactive control of 3D class-A Bézier curves. In *SIGGRAPH ASIA, Sketches*, 2008.
- [8] T. Harada. Study of quantitative analysis of the characteristics of a curve. *FORMA*, 12(1):55–63, 1997.
- [9] T. Harada and M. M. F. Yoshimoto. An aesthetic curve in the field of industrial design. In *Proceedings of IEEE Symposium on Visual LanguagesA*, pages 38–47, 1999.
- [10] M. Higashi and M. H. K. Kaneko. Generation of high quality curve and surface with smoothly varying curvature. *Eurographics*, pages 79–92, 1998.
- [11] P. Joshi and C. Séquin. Energy minimizers for curvature-based surface functionals. *Computer Aided Design and Applications*, 4(5):607–617, 2007.
- [12] R. Levien and C. H. Séquin. Interpolating splines: Which is the fairest of them all? *Computer Aided Design and Applications*, 6(1):91–102, 2009.
- [13] K. T. Miura. A general equation of aesthetic curves and its self-affinity. *Computer-Aided Design and Applications*, 3(1–4):457–464, 2006.
- [14] H. P. Moreton and C. H. Séquin. Functional optimization for fair surface design. In *Computer Graphics (Proceedings of SIGGRAPH 92)*, pages 167–176, jul 1992.
- [15] J. A. Nelder and R. Mead. A simplex method for function minimization. *Computer Journal*, 7:308–313, 1965.
- [16] Y. Wang, B. Zhao, L. Zhang, J. Xu, K. Wang, and S. Wang. Designing fair curves using monotone curvature pieces. *Computer Aided Geometric Design*, 21(5):515–527, 2004.
- [17] N. Yoshida, T. Hiraiwa, and T. Saito. Interactive control of planar class a bézier curves using logarithmic curvature graphs. *Computer-Aided Design and Applications*, 5(1–4):121–130, 2008.
- [18] N. Yoshida and T. Saito. Interactive aesthetic curve segments. *The Visual Computer (Proc. of Pacific Graphics)*, 22(9–11):896–905, 2006.
- [19] N. Yoshida and T. Saito. Quasi-aesthetic curves in rational cubic bézier forms. *Computer-Aided Design and Applications*, 4(1–4):477–486, 2007.